NAVAL POSTGRADUATE SCHOOL
MONTEREY, CALIFORNIA

THESIS

RADIATED POWER CONTROL
FOR
NARROW-BAND DIGITAL LINKS

by

Hsien-Ming Hsu

March, 1996

Thesis Advisor: Chin-Hwa Lee

Approved for public release; distribution is unlimited.

DISCLAIMER NOTICE

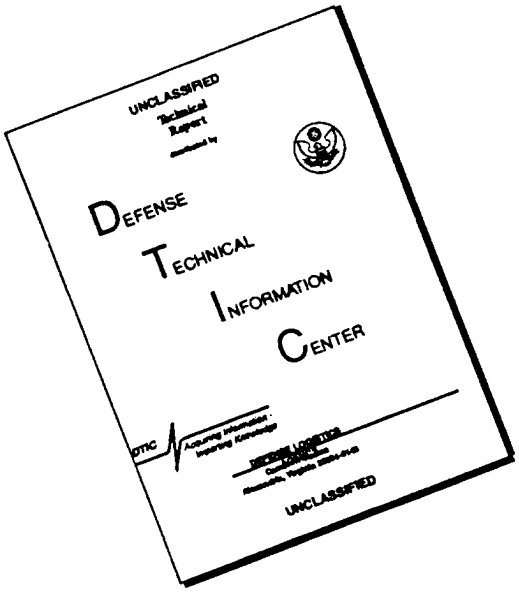

THIS DOCUMENT IS BEST QUALITY AVAILABLE. THE COPY FURNISHED TO DTIC CONTAINED A SIGNIFICANT NUMBER OF PAGES WHICH DO NOT REPRODUCE LEGIBLY.

REPORT DOCUMENTATION PAGE

Form Approved OMB No.0704-0188

1. AGENCY USE ONLY (*Leave blank*)	2. REPORT DATE March, 1996	3. REPORT TYPE AND DATES COVERED Master's Thesis

4. TITLE AND SUBTITLE

RADIATED POWER CONTROL FOR NARROW-BAND DIGITAL LINKS

5. FUNDING NUMBERS

6. AUTHOR(S) Hsien-Ming Hsu

7. PERFORMING ORGANIZATION NAME(S) AND ADDRESS(ES)
Naval Postgraduate School
Monterey CA 93943-5000

8. PERFORMING ORGANIZATION REPORT NUMBER

9. SPONSORING/MONITORING AGENCY NAME(S) AND ADDRESS(ES)

10. SPONSORING/MONITORING AGENCY REPORT NUMBER

11. SUPPLEMENTARY NOTES The views expressed in this thesis are those of the author and do not reflect the official policy or position of the Department of Defense or the U.S. Government.

12a. DISTRIBUTION/AVAILABILITY STATEMENT Approved for public release; distribution unlimited

12b. DISTRIBUTION CODE

13. ABSTRACT (*maximum 200 words*)

Radiated power control is one way to increase the capacity of a narrow-band channel with channel reuse. But channel reuse introduces the problem of co-channel interference. Use of a power control algorithm not only can optimize the radiated power for a particular quality of service (QOS) but also minimize co-channel interference at the receiver.

In this thesis, we present the experimental results that relate the dependency of the logarithm of bit error rate (BER) versus the logarithm of the ratio of the energy per bit to the one-sided noise power spectral density (E_b/N). The dependency of BER to E_b/N_0 in an ideal and to E_b/N in a nonideal thermal noise limited receiver were analyzed. One important step in the analysis is the procedure of curve fitting used to characterize the radiated power for a particular system. In addition, we perform the experiments of BER measurement with a fixed power at a fixed location and the experiment to obtain the relationship between BER and the transmission distance with fixed radiated power. A curve fitting procedure to find the selected system parameter ρ is based on the results of BER measurement at a fixed distance with variable power. The fixed step power control algorithm is also presented here. Experimental results are shown and compared to results expected from theory.

14. SUBJECT TERMS radiated power control, narrow-band, bit error, BER, quality of service	15. NUMBER OF PAGES 68
	16. PRICE CODE

17. SECURITY CLASSIFICATION OF REPORT	18. SECURITY CLASSIFICATION OF THIS PAGE	19. SECURITY CLASSIFICATION OF ABSTRACT	20. LIMITATION OF ABSTRACT
Unclassified	Unclassified	Unclassified	UL

NSN 7540-01-280-5500

Standard Form 298 (Rev. 2-89)
Prescribed by ANSI Std. 239-18

Approved for public release; distribution is unlimited.

RADIATED POWER CONTROL
FOR
NARROW-BAND DIGITAL LINKS

Hsien-Ming Hsu
Lieutenant Commander, Republic of China, Taiwan Navy
B.S., Naval Postgraduate School, 1995

Submitted in partial fulfillment
of the requirements for the degree of

MASTER OF SCIENCE IN ELECTRICAL ENGINEERING

from the

NAVAL POSTGRADUATE SCHOOL
March 1996

Author: _____
Hsien-Ming Hsu

Approved By: _____
Chin-Hwa Lee, Thesis Advisor

_____
R. Clark Robertson, Second Reader

_____
Herschel H. Loomis Jr., Chairman
Department of Electrical and Computer Engineering

ABSTRACT

Radiated power control is one way to increase the capacity of a narrow-band channel with channel reuse. But channel reuse introduces the problem of co-channel interference. Use of a power control algorithm not only can optimize the radiated power for a particular quality of service (QOS) but also minimize co-channel interference at the receiver.

In this thesis, we present the experimental results that relate the dependency of the logarithm of bit error rate (BER) versus the logarithm of the ratio of the energy per bit to the one-sided noise power spectral density (E_b/N). The dependency of BER to E_b/N_0 in an ideal and to E_b/N in a nonideal thermal noise limited receiver were analyzed. One important step in the analysis is the procedure of curve fitting used to characterize the radiated power for a particular system. In addition, we perform the experiments of BER measurement with a fixed power at a fixed location and the experiment to obtain the relationship between BER and the transmission distance with fixed radiated power. A curve fitting procedure to find the selected system parameter ρ is based on the results of BER measurement at a fixed distance with variable power. The fixed step power control algorithm is also presented here. Experimental results are shown and compared to results expected from theory.

TABLE OF CONTENTS

ACKNOWLEDGEMENTS

I wish to express my gratitude to my thesis advisor Professor Chin-Hwa Lee for his guidance and assistance in the completion of this thesis.

I would also like to express my appreciation to Professor R. Clark Robertson for taking the time and effort to by my second reader, and to others who contributed their assistance in the accomplishment of this thesis.

Finally, I am most grateful for my family, whose love and affection have been the force that helped me to achieve this educational goal.

I. INTRODUCTION

Usually a radio transmitter has a fixed radiated power. When a transmitter is operating over a specific channel, no other transmitter within the radiation area can transmit over the same channel without significant mutual interference occuring. Power control of transmitted power is one way to increase the capacity of a narrow-band channel with frequency reuse. Power control allows multiple users at different locations to communicate on the same frequency channel at the same time. But channel reuse introduces another problem, that of co-channel interference. The power control algorithm (PCA) can optimize the radiated power of transmitters utilizing the same frequency channel for a particular quality of service (QOS) and minimize the co-channel interference at each receiver.

In Kumar, Yates and Holtsman [Ref. 1], a simple distributed algorithm for power control based on bit-error-rate (BER) measurements were presented. It was designed for the reverse link of a DS/CDMA system to achieve specified BERs, which were more readily measurable than the signal-to-interference ratios (SIR). In an earlier paper [Ref. 2], the performance of handoff algorithms using both BER and relative signal strength measurements were analyzed. The algorithm performs a handoff only if the current BER performance is not adequate and if the relative signal strength of the new base station exceeds the signal strength from the present base station by a certain level. In Chockalingam and Milstein [Ref. 3], the power control error statistics and average

bit-error performance of a closed-loop power control scheme in a Rayleigh fading environment were presented. The effects of various loop parameters were analyzed as well. The power control examined in this thesis does not involve handoff to other base stations. Instead, power control is used to maintain a minimum link quality.

The goal of this thesis is to design a fixed step, closed loop power control algorithm based on the measured BER to regulate transmitted power for a narrow-band digital link. The procedure of "curve fitting" to characterize the radiated power for a particular system at fixed distance is introduced. Here, system parameter ρ is used to characterize the system in the experiments which will be explained in Chapter III.

The remainder of this thesis is organized as follows. In Chapter II, we describe the setup of the system and the components. In Chapter III, the probability of bit error for a digital link with thermal noise and unknown interference is introduced; then, we describe the curve fitting procedure to find the system parameter ρ. In Chapter IV, experimental results for BER at a fixed distance with a fixed radiated power and interference present are discussed. The BER measurement at variable distance with fixed power are described as well. We use data from BER measurements with variable radiated power both with and without jamming noise at a fixed distance to find the system parameter ρ. Then, we describe the fixed step power control algorithm used in the experiment and show the results. All of experiments are performed on the roof top of Spanagel Hall of Naval Postgraduate School. In Chapter V, we discuss practical problems associated with the experiment. Conclusions are presented in Chapter VI.

II. THE EXPERIMENTAL SYSTEM AND COMPONENTS

The transmitter and receiver systems employed for our experiments with a digital narrow-band link are discribed in the following. The transmitter, shown in Figure 2.1, contains a Terminal Node Controller (TNC), the Kantronics data engine and Kantronics DE19K2/9K modem, and a Kantronics D4-10 UHF Wide-Band Transceiver. A digital step attenuator and a fixed attenuator reduce the power to the antenna. Two PC computers are used in the transmitter. The receiver shown in Figure 2.2 contains the TNC Kantronics data engine and Kantronics DE19K2/9K6 modem, a Kantronics D4-10 UHF Wide-Band Transceiver, a bandpass cavity filter, an error counter, a DAQPad-1200 data acquisition system, and the antenna. Two PC computers are also used in the receiver. The components used in the transmitter and receiver are discussed in more detail in the following subsections.

A. KANTRONICS DATA ENGINE

The Kantronics data engine is a Terminal Node Controller (TNC). It supports the Amateur Radio Packet AX.25, Version 2, Level 2, protocol adopted by the American Radio Relay League. It can receive a digital message stream from a computer and convert it to an audio signal suitable for transmission. It can also receive an audio signal from a transceiver and convert the audio signal to a digital signal for a computer. The TNC link layer software converts data into packets, adds the required addressing,

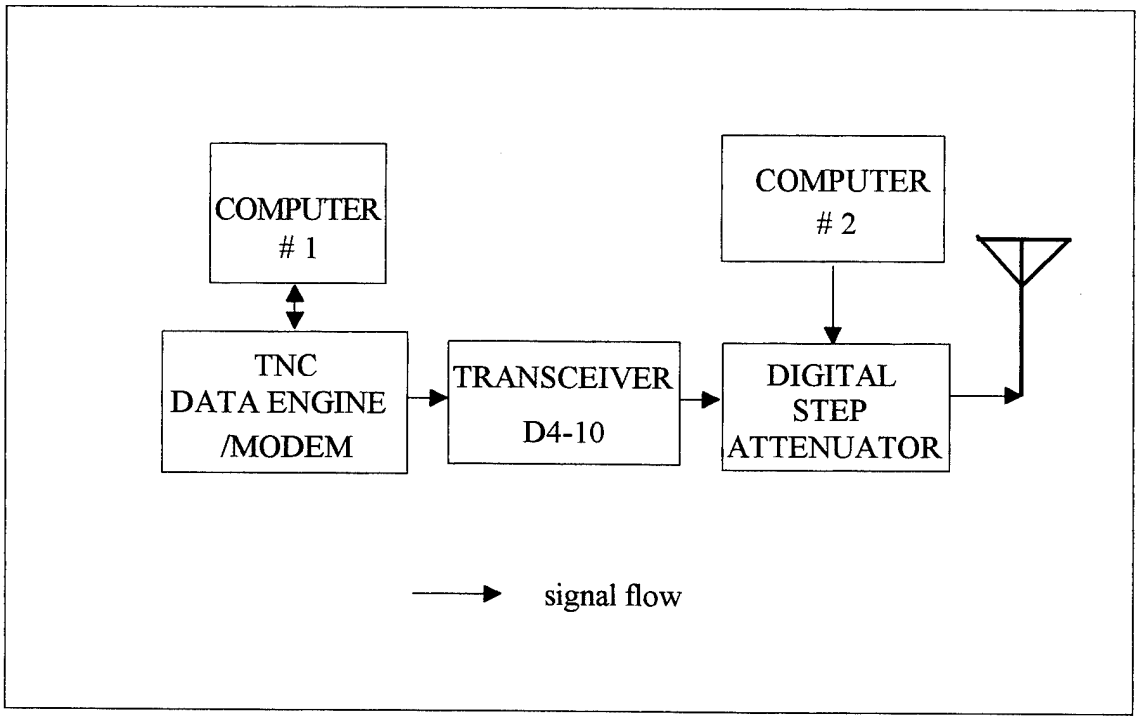

Figure 2.1. Transmitter Block Diagram

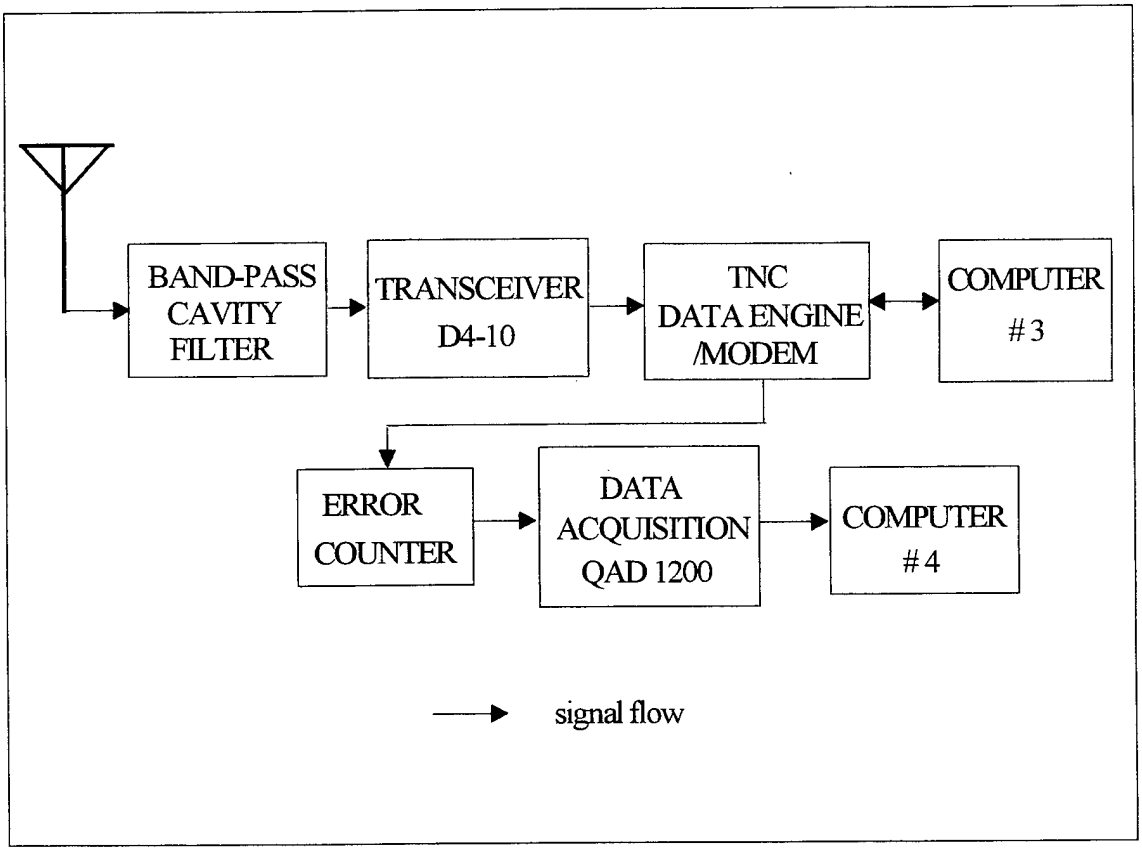

Figure 2.2. Receiver Block Diagram

error checking, and control information to insure that the data gets from one Node to the next. The error checking implemented in the TNC is the same as the error checking used by other stations following the AX.25 Standard [Ref. 4].

B. KANTRONICS DE19K2/9K6 MODEM

The Kantronics DE19K2/9K6 modem, also known as radio modem, is a direct frequency-shift-keying (DFSK) modem capable of operating at either 9600 or 19200 baud [Ref. 5]. The DE19K2/9K6 modem incorporates a BERT (Bit Error Rate Test) mode that allows bit error rate measurements. The experiments conducted in this thesis rely on this mode. The transceiver used with this modem at 19200 baud rate requires a wideband receiver with an intermediate frequency of 60 KHz minimum. Also required is a linear-phase filter with gaussian response and a threshold detector with a transistor-transistor logic (TTL) output connected to the receive data line (RXD). In the transmitter, a frequency deviation of -10 KHz is defined as a TTL low and +10 KHz is defined as a TTL high.

C. KANTRONICS D4-10 UHF WIDE-BAND TRANSCEIVER

The Kantronics D4-10 transceiver provides a 10-watt output for high-speed packet operation on the UHF (440 MHz) amateur band. The transmitter has been modified to generate power less than 1-watt for short range operation. Unique features of the Kantronics D4-10 are selection of narrow or wide bandwidth reception, narrow

narrow or wide transmit deviation settings, fast transmitter-receiver (TR) switching, analog and TTL modem interfacing, direct transmit varicap access, direct discriminator access on receive, and receiver-derived carrier detect [Ref. 6].

D. DIGITAL STEP ATTENUATOR

The digital step attenuator contains six TTL control input pins which select either 0.5, 1, 2, 4, 8 or 16 dB attenuation either separately or in combination. The different attenuations can be combined for a range of 64 steps from 0.5 dB to 31.5 dB. The attenuation can be controlled by a computer port or by manual digital switches. The operating range of the frequency is from 10 MHz to 1 GHz.

E. DIGITAL ERROR COUNTER

The purpose of the error counter is to count the number of errors during a collection period. The definition of an error is that a 0 state is received when a 1 state was sent by the transmitter. The digital error counter is a six-digit digital counter, and its range is from 0 to 999999. There is a push button to reset the digital counter and a disable/enable switch. The counter is built from programmable logic chips, and the program is shown in the Appendix.

F. DAQPAD-1200 DATA ACQUISITION SYSTEM

The DAQPad-1200 is made by NATIONAL INSTRUMENTS INC. It is a low-cost, multi-function I/O DAQ unit that communicates with the PC through a parallel port. The DAQPad-1200 has a 12-bit ADC with eight analog inputs, configurable as eight single-ended or four differential inputs; two 12-bit DACs with voltage outputs; 24 lines of TTL-compatible digital I/O; and three 16-bit counter/timer for timing I/O. It is used to collect error counter information for the PC. Only 24 I/O lines were used in this experiment. The DAQPad-1200 is completely software configurable and self-calibrated.

G. CAVITY BANDPASS FILTER

The model WP-469-1 bandpass cavity was made by WACOM PRODUCTS, INC. It is a high performance model designed for use in systems that require greater selectivity than that provided by smaller diameter filters. The superiority of this high performance filter is particularly noticeable when the frequency to be attenuated is relatively close to the frequency to be passed. The bandpass cavity is designed for use between the antenna and the receiver or between the antenna and the transmitter to reduce interference. The bandpass cavity is a 10 inch one-quarter wavelength coaxial cavity filter designed for use with transmitters or receivers operating in the 406 - 420 MHz band.

H. PERSONAL COMPUTER

There are four 486DX PCs in this system. Number 1 and number 2 are used at transmitter side, and number 3 and number 4 are used at the receiver side. Number 1 and number 3 PCs check messages formatted as A.25s. Number 2 and number 4 PCs perform the power control algorithm which is written in LABVIEW software. The collection period for BER measurement is set in this software package.

I. ANTENNA

The Helical KD4-440 model antenna used at the transmitter and receiver site is approximately 6 inches in length and made by LARSEN, INC. Its center frequency is designed to be 440 MHz for 70 centimeters wavelength range. The antenna is a helical antenna with unity gain, an input impedance of 50 ohms, and is 1/4 wavelength long at 440 MHz. The allowable radiated power is 25 watt.

III. THEORETICAL BACKGROUND AND PROCEDURES FOR EXPERIMENTS

In this chapter, we introduce the probability of bit error with unknown interference. Here, the equations include the probability of bit error for noncoherent detection of FSK in an ideal thermal noise limited receiver and a nonideal noisy receiver. These formulas will be used to interpret the results of the experiments described in the next chapter. Based on the measured experimental results and the curve of the probability of bit error for noncoherent detection of FSK in a thermal noise limited receiver, we can find the system parameter ρ by a curve fitting procedure. In the second section, we describe the details of the curve fitting procedure.

A. THE PROBABILITY OF BIT ERROR WITH UNKNOWN INTERFERENCE

In a digital receiver the probability of bit error P_e at the detector output is used to describe the quality of the recovered signal. The P_e is a function of the ratio of the energy per bit E_b to the one-sided noise power spectral density N_0. In an ideal thermal noise limited receiver, E_b/N_0 measured at the detector input determines the detection quality [Ref.8]. The E_b/N_0 in decibels received at the detector input in a digital communication system is related to the link parameters by

$$\left(\frac{E_b}{N_0}\right)_{dB} = (P_{EIRP})_{dB} - (L_{FS})_{dB} + \left(\frac{G_{AR}}{T_0}\right)_{dB} - k_{dB} - R_{dB} \tag{3.1}$$

In ratio form, this is equivalent to

$$\left(\frac{E_b}{N_0}\right) = \frac{P_{EIRP}G_{AR}}{L_{FS}T_0kR} \tag{3.2}$$

where

E_b: energy per bit

N_0: noise spectral density

$(P_{EIRP})_{dBW} = 10\log(P_{EIRP})$ is the effective isotropic radiated power of the transmitter in dB above 1W. $(P_{EIRP})_{dBW} = (P_{TX} + G_{AT})_{dBW}$

P_{TX} : is the signal power into the transmitting antenna

G_{AT}: the transmitting antenna gain

G_{AR}: the receiving antenna gain

$(L_{FS})_{dB}$: the path loss. For a fixed propagation distance this is assumed to be constant

T_0: equivalent room temperature or 290 K

k_{dB}: $10\log(1.38*10^{-23}) = -228.6$ dB where k is Boltzmann's constant

R_{dB}: $10\log(R)$ and R is the data rate (bits/second)

In a nonideal, noisy receiver E_b/N determines the detection quality where

$$\left(\frac{E_b}{N}\right)_{dB} = [(P_{TX} + G_{AT})_{dB} - (L_{FS})_{dB} + (\frac{G_{AR}}{T_{syst}})_{dB} - k_{dB} - R_{dB}] \tag{3.3}$$

This is equivalent to

$$\left(\frac{E_b}{N}\right) = \frac{P_{TX}G_{AT}G_{AR}}{kL_{FS}T_0(NF)R} \tag{3.4}$$

where

T_{syst} : the receiving system equivalent noise temperature (K)

$T_{syst} = T_e + T_0 = T_0(NF)$

NF : system noise figure

From equations 3.1 and 3.3, we get

$$\left(\frac{E_b}{N}\right)_{dB} = \left(\frac{E_b}{N_0}\right)_{dB} - (NF)_{dB} \tag{3.5}$$

The bit error rate (BER) for noncoherent detection of an FSK signal in an ideal thermal noise limited receiver is

$$P_b = P_b\left[\left(\frac{E_b}{N_0}\right)\right] = \frac{1}{2}e^{-\frac{1}{2}\left(\frac{E_b}{N_0}\right)} = \frac{1}{2}e^{-\frac{1}{2}\left(\frac{G_{AT}G_{AR}}{L_{FS}T_0kR}\right)P_{TX}} \tag{3.6}$$

If we define

$$\beta = \frac{G_{AT}G_{AR}}{L_{FS}T_0kR} \tag{3.7}$$

then equation 3.6 can be expressed as

$$P_b = \frac{1}{2}e^{-\frac{1}{2}\beta P_{TX}} \tag{3.8}$$

In order to see the dependency of the logarithm of BER versus the logarithm of (E_b/N_0), equation 3.6 and 3.8 can be written as

$$\log_e P_b = -\ln 2 - \frac{1}{2}10^{0.1\left(\frac{E_b}{N_0}\right)_{dB}} = -\ln 2 - \frac{1}{2}10^{0.1\left(\beta_{dB}+(P_{TX})_{dB}\right)} \tag{3.9}$$

The bit error rate (BER) for noncoherent detection of FSK in a noisy receiver is

$$P'_b = P'_b\left[\left(\frac{E_b}{N}\right)\right] = \frac{1}{2}e^{-\frac{1}{2}\left(\frac{E_b}{N}\right)} = \frac{1}{2}e^{-\frac{1}{2}\left(\frac{G_{AT}G_{AR}}{L_{FS}T_0kR}\right)\left(\frac{P_{TX}}{NF}\right)} \tag{3.10}$$

which can be simplified to obtain

$$P_b' = \frac{1}{2}e^{-\frac{1}{2}\beta\left(\frac{P_{TX}}{NF}\right)} \tag{3.11}$$

To express the dependency of logarithm of BER versus logarithm of (E_b/N), equation 3.10 and 3.11 can be written as

$$\log_e P_b' = \log_e\left(\frac{1}{2}e^{-\frac{1}{2}\left(\frac{E_b}{N}\right)}\right) = -\ln 2 - \frac{1}{2}10^{0.1\left[\left(\frac{E_b}{N_0}\right)_{dB} - (NF)_{dB}\right]} \tag{3.12}$$

This is equivalent to

$$\log_e P_b' = -\ln 2 - \frac{1}{2}10^{0.1\left[\beta_{dB} + (P_{TX})_{dB} - (NF)_{dB}\right]} \tag{3.13}$$

Therefore, from equations 3.9 and 3.13

$$P_b'\left[\left(\frac{E_b}{N}\right)_{dB}\right] = P_b\left[\left(\frac{E_b}{N_0}\right)_{dB} - (NF)_{dB}\right] \tag{3.14}$$

The BER of a noisy receiver is actually a shifted function of the BER of an ideal thermal noise limited receiver along the logarithm scale of (E_b/N_0). In the experiment, we change P_{TX} by adding attenuation. Hence, we have

$$\beta_{dB} + (P_{TX})_{dB} = \alpha - (L_i)_{dB} \tag{3.15}$$

where

α : the transmitted power

$(L_i)_{dB}$: digital step attenuation in dB

Therefore, for an ideal thermal noise limited receiver equation 3.8 becomes

$$\log_e P_b = -\ln 2 - \frac{1}{2}10^{0.1\left(\alpha - (L_i)_{dB}\right)} \tag{3.16}$$

For a noisy receiver equation 3.13 becomes

$$\log_e P'_b = -\ln 2 - \tfrac{1}{2} 10^{0.1\left[\alpha - (Li)_{dB} - (NF)_{dB}\right]} \tag{3.17}$$

Let

$$\rho = \alpha - (NF)_{dB} \tag{3.18}$$

Then equation 3.17 is equivalent to

$$\log_e P'_b = -\ln 2 - \tfrac{1}{2} 10^{0.1\left[\rho - (L_i)_{dB}\right]} \tag{3.19}$$

The symbol ρ is a parameter that characterizes a particular radio over a fixed distance transmission. In order to characterize the system in our experiments it is necessary to obtain ρ from experimental data.

B. CURVE FITTING TO FIND THE PARAMETER ρ

In order to do power control, it is necessary to characterize the radios in terms of the parameters ρ. Due to many interference possibilities in the experiments, it is very difficult to obtain ρ from the experimental data directly. However, we can get ρ by fitting the measured samples of P'_b with the curve of P_b in a minimum mean square sense, as shown in Figure 3.1 and Figure 3.2. The following is the procedure used to find ρ.

Step 1: In the experiments, we reduce the radiated power by L_i (dB) using the digital step attenuator as shown in Figure 3.1. We collect n samples of the curve of P'_{bi} (BER_i, L_i).Then from equation 3.19

$$BER_i = P'_{bi} = \frac{1}{2}e^{-\frac{1}{2}\rho_i} \qquad i = 1,2,3,\ldots,n \tag{3.20}$$

where

$$(\rho_i)_{dB} = \rho - (L_i)_{dB} \tag{3.21}$$

ρ_i: the radiated power

BER_i: the ith bit error rate sample measured

and

$$BER_i = \begin{bmatrix} BER_1 \\ BER_2 \\ \vdots \\ BER_n \end{bmatrix} \tag{3.22}$$

The problem is to determine the value of ρ. Assume an arbitrary initial ρ value. Based on the measured BER_i, the radiated power with different attenuations ρ_i can be calculated as

$$\rho_i = \begin{bmatrix} \rho - L_1 \\ \rho - L_2 \\ \vdots \\ \rho - L_n \end{bmatrix} \tag{3.23}$$

Step 2: Obtain the corresponding probability of error P'_b by using the calculated ρ_i from equation 3.23 in equation 3.19. From equations 3.14, we see that the P'_b curve of a noisy receiver is a shifted version of the P_b curve of an ideal thermal noise limited receiver. For the given ρ_i, we wish to obtain P_b. Equation 3.16 becomes

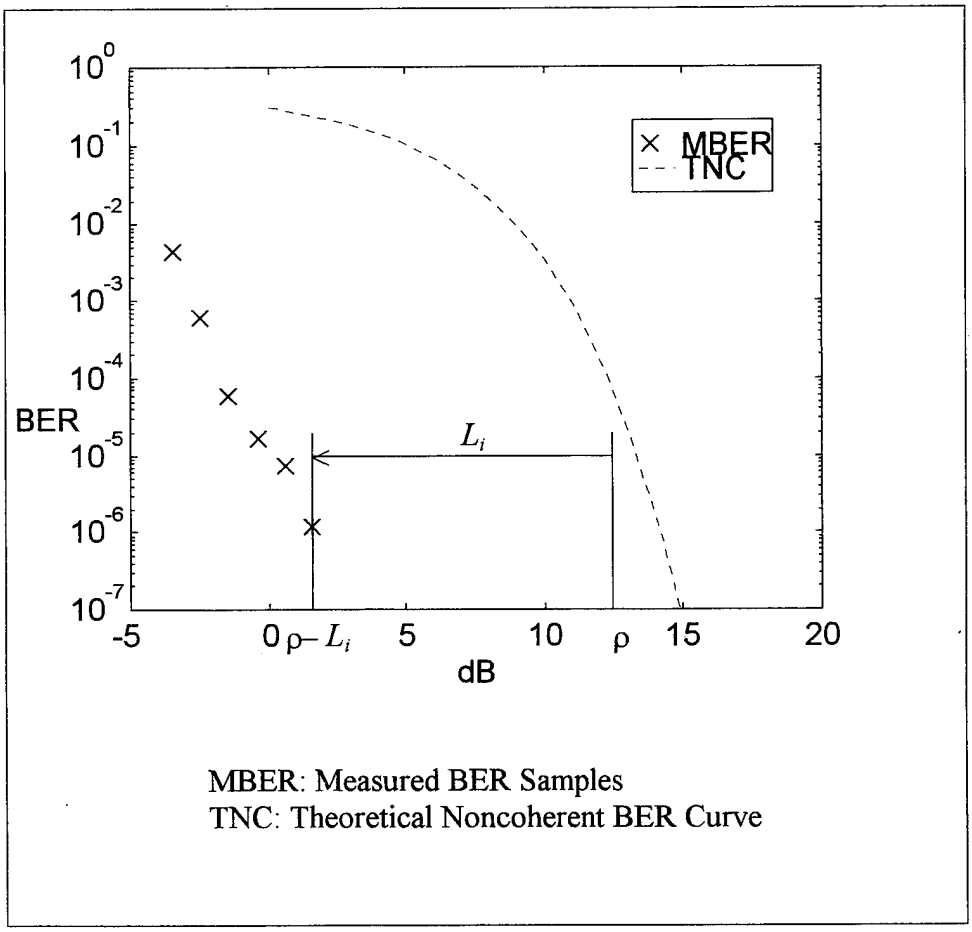

Figure 3.1. Measured BER Samples Versus the ρ Changed by L_i.

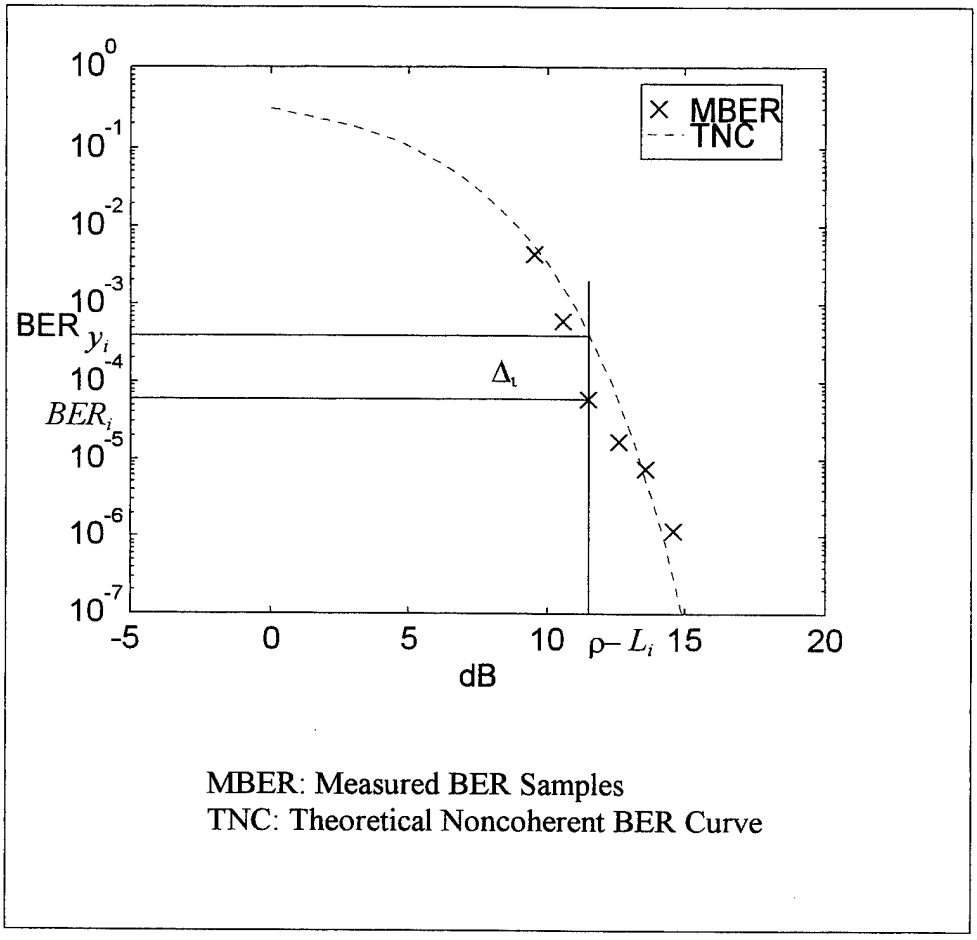

Figure 3.2. Move the Measured BER Samples Until the Mean Square Error Is Minimum.

$$y_i = P_b = \frac{1}{2}e^{-\frac{1}{2}x_i} \tag{3.24}$$

where

x_i : the n values of E_b/N_0 from equation 3.24.

y_i : the probability of bit error for an ideal receiver

There are n x_i values along the horizontal axis of the P_b curve.

From Equation 3.24, we obtain the y_i:

$$y_i = \begin{bmatrix} y_1 \\ y_2 \\ \vdots \\ y_n \end{bmatrix} \tag{3.25}$$

Step 3: Calculate the difference between y_i and BER_i as shown in Figure 3.2.

We subtract equation 3.25 from equation 3.22 to obtain

$$\Delta_i = (BER_i - y_i) = \begin{bmatrix} \Delta_1 \\ \Delta_2 \\ \vdots \\ \Delta_n \end{bmatrix} \tag{3.26}$$

Step 4: Finally, we search for an appropriate ρ so that

$$\min \left\{ \Sigma_1^n \Delta_i^2 \right\} \tag{3.27}$$

is achieved. In practice, we have found that n = 6 yields sufficiently accurate results.

IV. THE EXPERIMENTAL RESULTS

The goal of these experiments is to find the system parameter ρ. Before designing the power control algorithm, we need to investigate the response of BER with FM jamming noise present. In this chapter, experiments to find the relationships among BER, distance, radiated power, and the system parameter ρ are described. To examine the sensitivity of the system parameter ρ, it is useful to add different levels of FM jamming power to the system. The results are checked to match the theoretical derivation shown in Chapter III. Finally, experimental results obtained for a fixed step power control algorithm are described.

A. INTERFERENCE PATTERN FOR BER AT FIXED DISTANCE WITH FIXED RADIATED POWER

Without knowing the status of the interference, we performed the BER measurement with a fixed power at a fixed distance (51.5 m). The results were expected to reveal some knowledge of interference status. The experimental result was shown in Figure 4.1. Each profile in Figure 4.1 represents an error count during a weekday. The collection period was around five minutes and was chosen depending on the desired error rate. Figure 4.2 shows the seven-day average data.

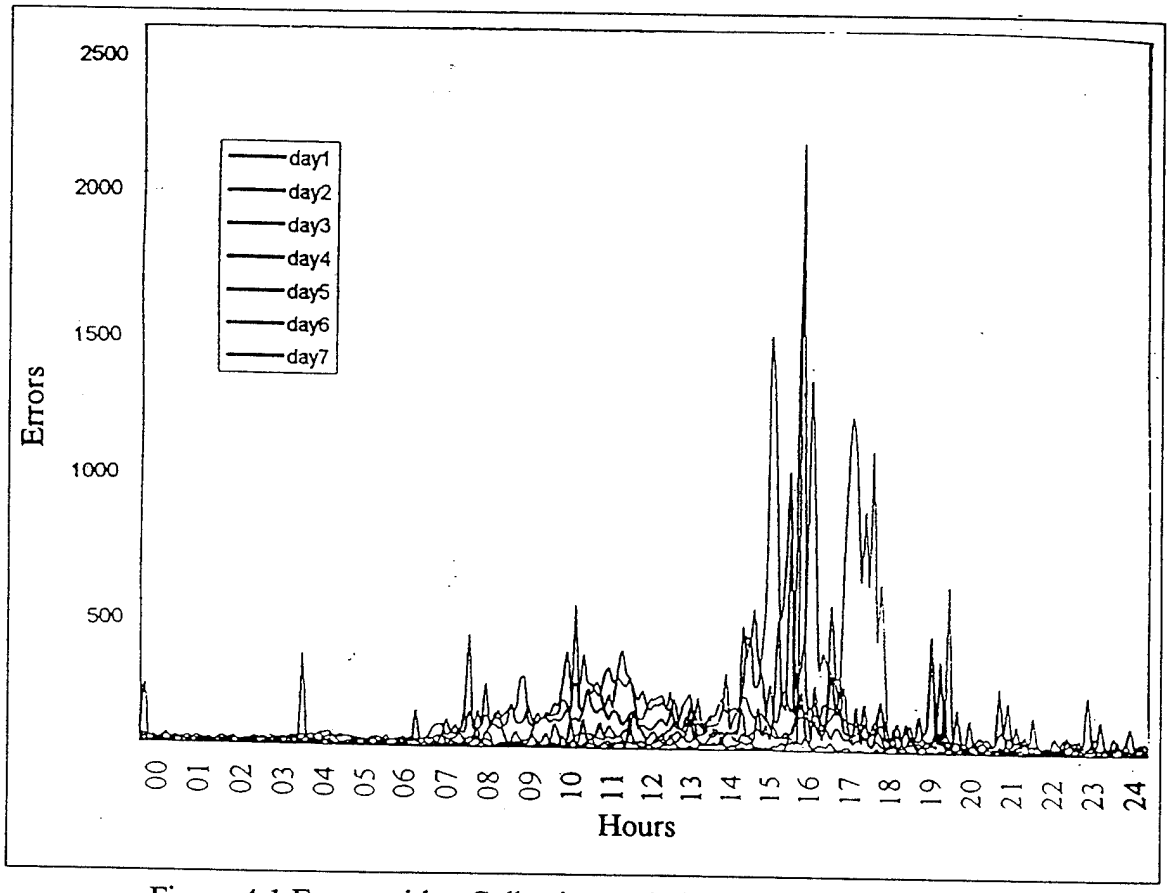

Figure 4.1 Errors with a Collection Period around 5 Minutes Versus 24 Hours for Seven Days.

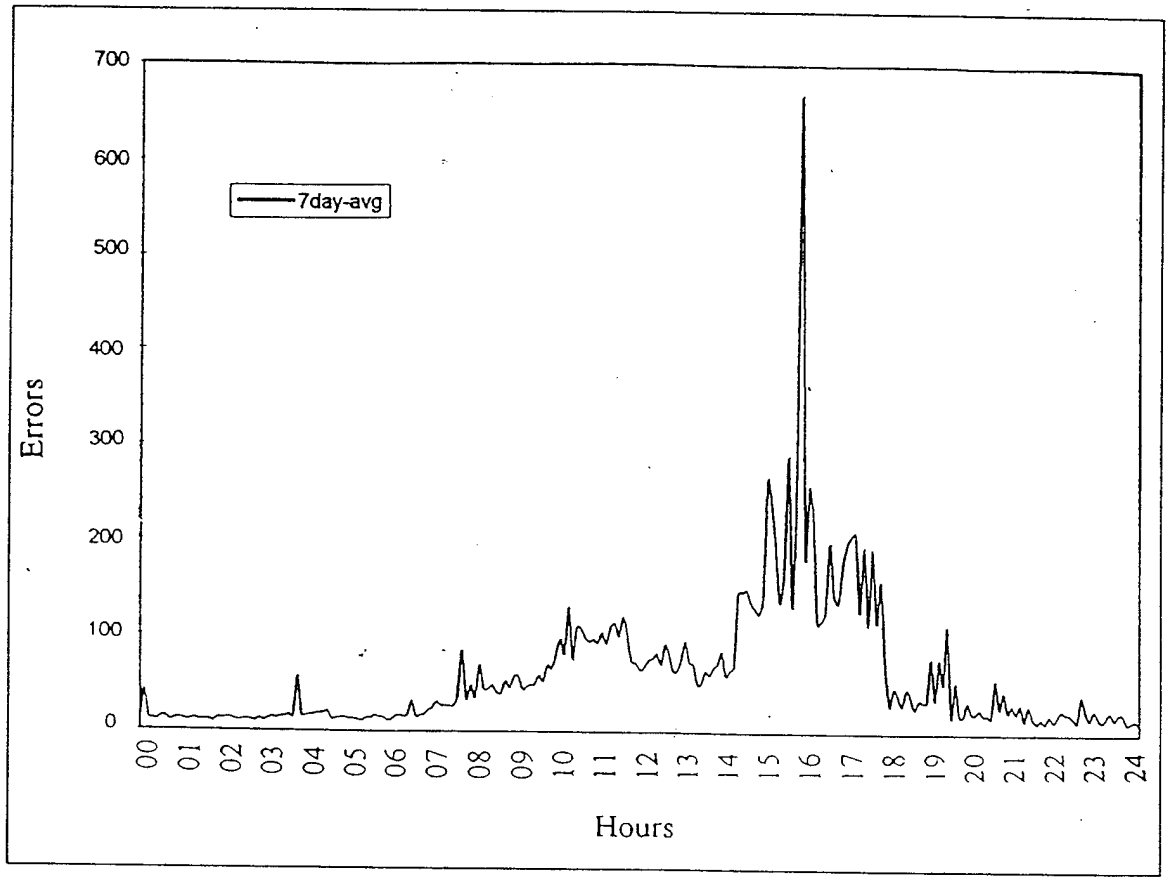

Figure 4.2 Seven-day Average Errors with the Collection Period Around 5 Minutes.

The counter does not measure errors in the receiver directly. The counter registers a number proportional to the errors from the received signal according to the following formula:

$$BER = \frac{N}{3TR} \tag{4.1}$$

where

N : the count from counter

T : the period of collection time (second) selected in LABVIEW software

R : Baud Rate = 19200 baud for this system

In an ideal communication environment, the profile for a whole day should be flat. Figure 4.1 shows that there are four periods of interference in each day. During work hours (0800 to 1700 hours), we see that the interference is the strongest. For some weekdays, this status is maintained until 7 PM. During the weekend, the strongest interference period is from 3 PM to 6 PM. A common observation for each day is that during the period from 0 AM to 8 AM the interference is the least.

Based on the results shown in Figures 4.1 and 4.2, a decision was made that the following experiments would be performed during the period of least interference (0000 hour to 0800 hour) in order to obtain more accurate results.

B. BER MEASUREMENT AT VARIABLE DISTANCE WITH FIXED POWER

The objective of this experiment is to find the relationship between BER and communication distance with fixed radiated power. From the results, we expect to obtain the relationship of signal strength variation measured in BER with distance. The relationship can then be used as a reference for the power change rate in a power control algorithm. Mean and standard deviation are shown in Figure 4.3. This figure shows the mean BERs and mean BERs$\pm$standard deviations for distances of 51.5m, 52m, 53.1m, 54.5m, and 56.72m.

In the same communication environment and based on equation 3.10, we expect the path loss L_{FS} to change for different distances. The mean BERs should increase with distance. Figure 4.3 does not show this phenomena because multipath interference on the roof top of Spanagel Hall is significant. Unavoidable interference destroys the relationship shown in Figure 4.3.

From this experiment, we learned that between two locations on the roof that the received BER is complicated because of unknown interference and multipath problems. If we perform this experiment in an anechoic chamber, we expect that the mean BER will increase with increasing distance. This negative conclusion suggests that varying distance in our experiments to obtain data is not a viable approach.

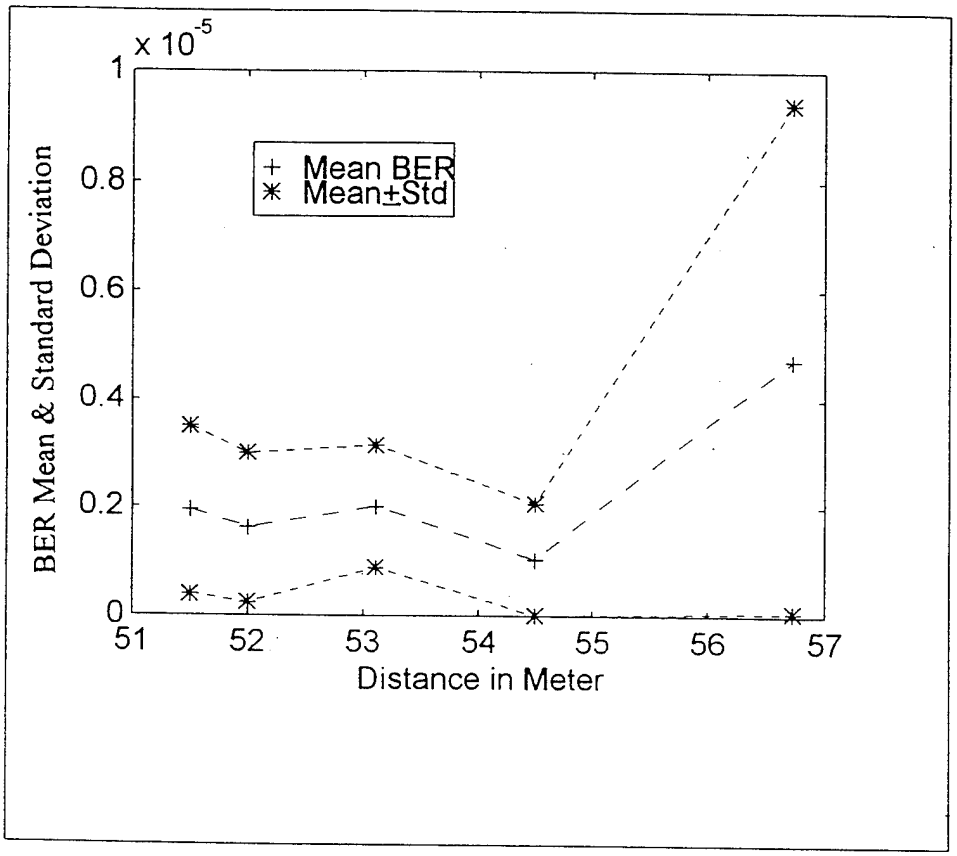

Figure 4.3 Measured Mean BER and Mean BER±Std Versus Five Locations with a Fixed Radiated Power.

C. FINDING PARAMETER ρ AND BER MEASUREMENT WITH VARIABLE RADIATED POWER AT FIXED DISTANCE

The objective of this experiment is to find the system parameter ρ from BER measurements with variable radiated power at fixed distance. Based on the results, we can judge whether this curve fitting procedure is viable or not. To avoid an error counter overflow in the experimental set up described previously, the distance between the transmitting antenna and the receiving antenna is set at 59.1 meters. Based on equation 3.20, six attenuations (L_i) were set on the digital step attenuator. We used a different collection period for each set of attenuations.

Three sets of data were collected in the experiments without jammer noise. The collection period, attenuation, and the measured mean BERs are shown in Tables 4.1, 4.2, and 4.3. Afterward, the measured mean BERs were used to find ρ via a curve fitting program written in GAMS (General Algebraic Modeling System) [Ref.7]. The program follows the steps and equations 3.18 to 3.25 discussed in the last Chapter.

Based on the data in Table 4.1, the parameter ρ is found to be 39.256 dBm and the mean square error (MSE) is equal to 2.76×10^{-8}. The measured BER samples adjusted using the results of the curve fitting procedure are shown in Figure 4.4.

i	1	2	3	4	5	6
L_i (dB)	29.23	28.22	27.26	26.17	25.21	24.2
collection period (sec)	20	30	60	90	360	600
measured mean BER	3.32×10^{-3}	7.31×10^{-4}	1.65×10^{-4}	8.16×10^{-5}	7.81×10^{-8}	4.91×10^{-6}
ρ (dBm)	39.256					
MSE	2.76×10^{-8}					

Table 4.1. Mean BER Measurement at Different Attenuation L_i (dB), and the System Parameter ρ from Curve Fitting

Based on the set of data shown in Table 4.2, the system parameter ρ is found to be 39.711 dBm, and the mean square error is 3.63×10^{-6}. The measured BER samples adjusted using the results of the curve fitting procedure are shown in Figure 4.5.

i	1	2	3	4	5	6
L_i (dB)	29.23	28.22	27.26	26.17	25.21	24.2
collection period (sec)	30	60	180	360	600	600
measured mean BER	2.18×10^{-5}	1.25×10^{-6}	1.09×10^{-6}	3.92×10^{-7}	1.09×10^{-7}	4.81×10^{-8}
ρ (dBm)	39.711					
MSE	3.63×10^{-3}					

Table 4.2. Mean BER Measurement at Different Attenuation L_i (dB), and the System Parameter ρ from Curve Fitting.

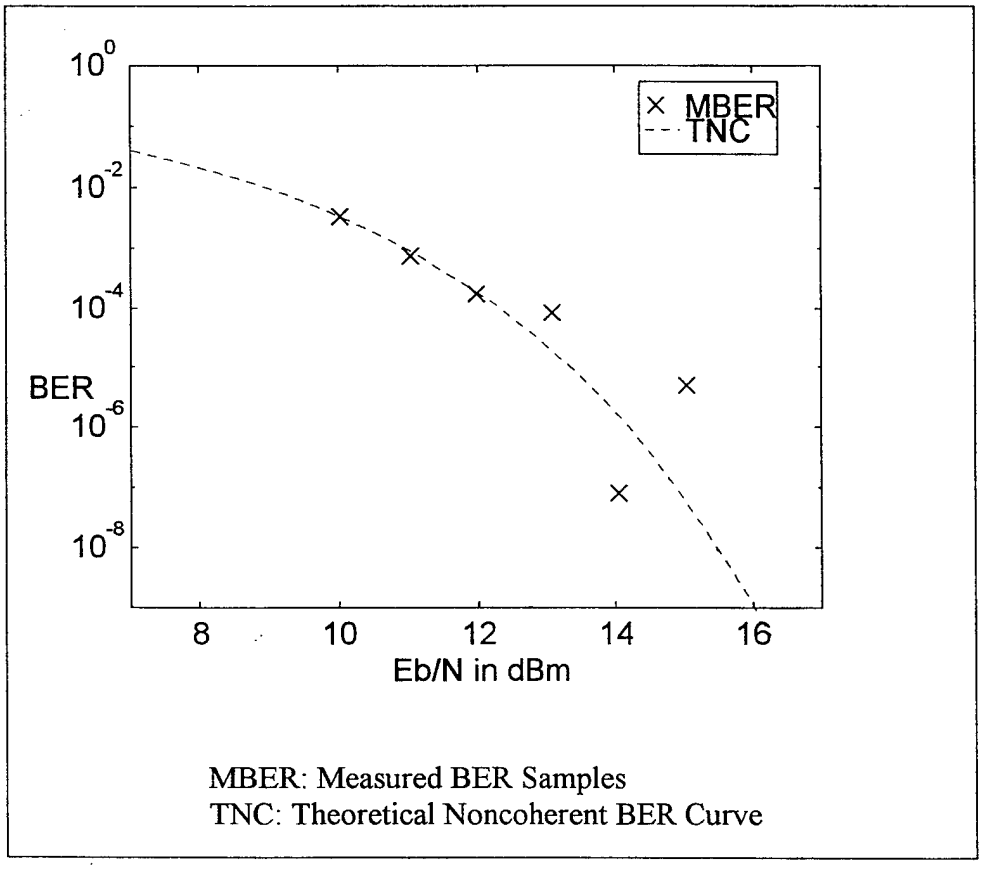

Figure 4.4. Measured BER Versus Variable Radiated Power with a Fixed Distance Compensated by System Parameter ρ.

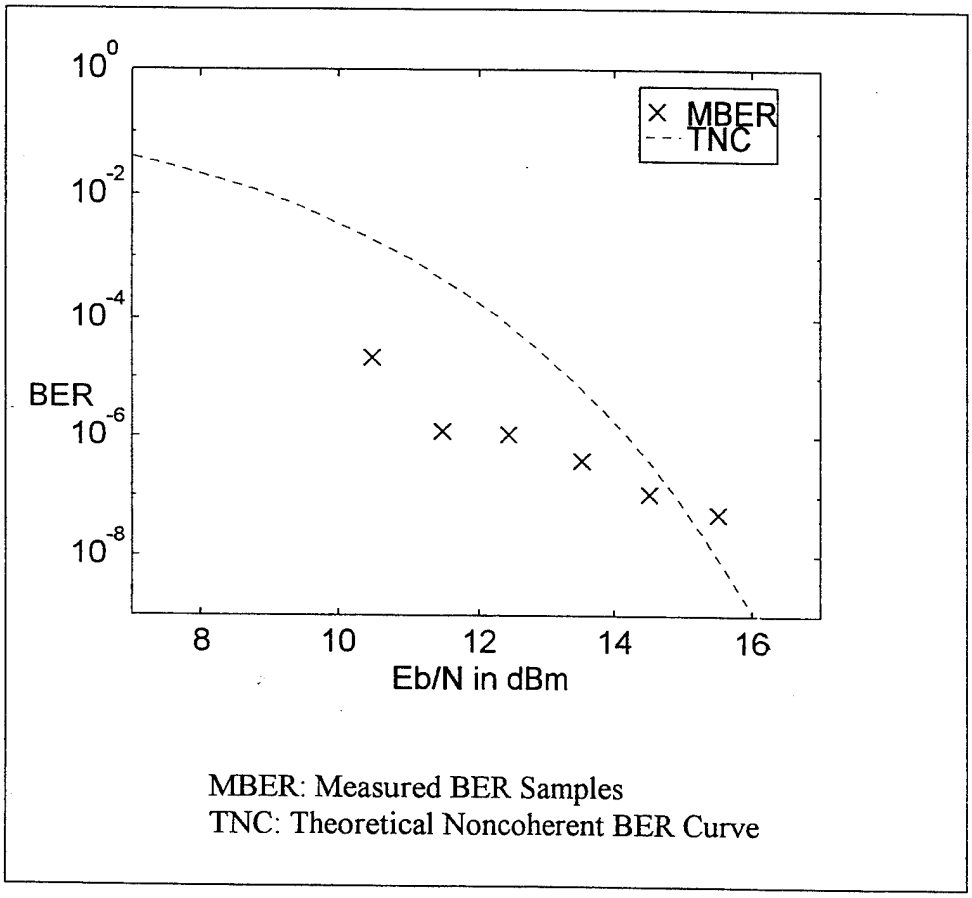

Figure 4.5 Measured BER Versus Variable Radiated Power with a Fixed Distance Compensated by System Parameter ρ.

Based on the set of data shown in Table 4.3, we obtain the system parameter ρ as 39.713 dBm, and the mean square error is 3.66×10^{-6}. The measured BER samples adjusted using the results of curve fitting procedure are shown in Figure 4.6.

i	1	2	3	4	5	6
L_i (dB)	29.23	28.22	27.26	26.17	25.21	24.2
collection period (sec)	120	180	120	360	600	600
measured mean BER	7.08×10^{-6}	7.69×10^{-6}	3.87×10^{-6}	5.88×10^{-9}	1.05×10^{-8}	1.10×10^{-5}
ρ (dBm)	39.713					
MSE	3.66×10^{-6}					

Table 4.3. Mean BER Measurement at Different Attenuation L_i (dB), and the System Parameter ρ from Curve Fitting.

If these experiments were performed with a thermal noise limited receiver in ideal conditions, the BERs should follow equation 3.6 and the mean square error should be equal to zero. However, these experiments were performed in a noisy environment. The parameter ρ's are around 39.5 dBm, and the maximum difference among ρ's is 0.457 dB which is less than 0.5 dB. Therefore, the curve fitting procedure a is very stable process by which to find the parameter ρ even in a noisy environment.

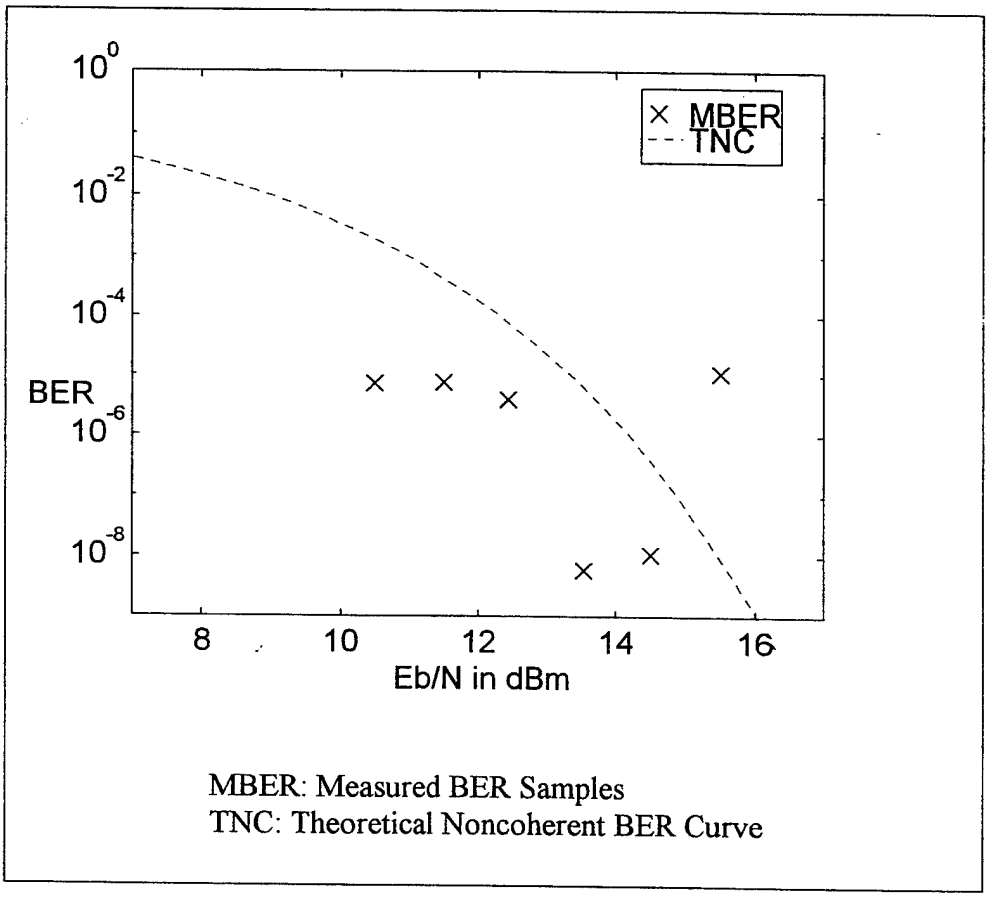

Figure 4.6. Measured BER Versus Variable Radiated Power with a Fixed Distance Compensated by System Parameter ρ.

D. FINDING THE SYSTEM PARAMETER ρ WITH JAMMER

To observe the response of the system parameter ρ, in the following experiments we added different amounts of jamming noise to the system. After the curve fitting procedure, we compared the results with the result predicted by equation 3.18. The jamming power added and the measured data are shown in Tables 4.4, 4.5, and 4.6. We repeated the experiment several times with different jamming powers. From these experiments we expect to learn how the parameter ρ is affected by different jamming powers. It is expected that the difference between different ρ's will be proportional to the difference between different jamming powers.

In Table 4.4 with a -18.5 dBm jamming power, the parameter ρ is found to be 38.788 dBm, and the mean square error is 1.390×10^{-6}. The measured BER samples adjusted using the results of curve fitting procedure are shown in Figure 4.7.

jamming power	-18.5 dBm					
i	1	2	3	4	5	6
L_i (dB)	29.23	28.22	27.26	26.17	25.21	24.2
collection period (sec)	20	30	60	90	360	600
measured mean BER	4.28×10^{-4}	5.86×10^{-4}	5.91×10^{-5}	1.68×10^{-5}	7.28×10^{-6}	1.15×10^{-6}
ρ (dBm)	38.388					
MSE	1.390×10^{-6}					

Table 4.4. Mean BER Measurement at Different Attenuation L_i (dB), and the System Parameter ρ from Curve Fitting.

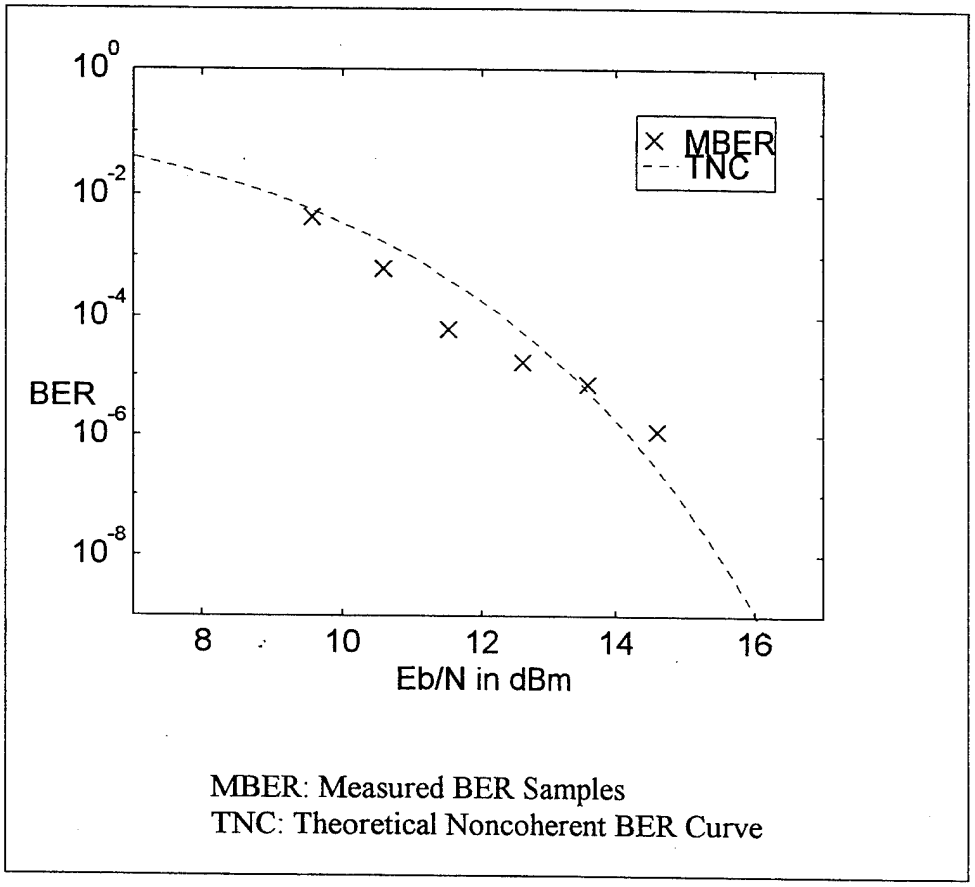

Figure 4.7. Measured BER Versus Variable Radiated Power with a Fixed Distance and a Fixed Jamming Power -18.5 dBm Compensated by System Parameter ρ.

In Table 4.5 with a -17.0 dBm jamming power, the parameter ρ is found to be 37.841 dBm, and the MSE is equal to 5.579×10^{-7}. The measured BER samples adjusted using the results of curve fitting procedure are shown in Figure 4.8.

jamming power	-17.0 dBm					
i	1	2	3	4	5	6
L_i (dB)	29.23	28.22	27.26	26.17	25.21	24.2
collection period (sec)	10	20	60	120	360	600
measured mean BER	1.23×10^{-2}	4.99×10^{-3}	1.56×10^{-3}	1.95×10^{-4}	8.87×10^{-6}	1.38×10^{-6}
ρ (dBm)	37.841					
MSE	5.579×10^{-6}					

Table 4.5. Mean BER Measurement at Different Attenuation L_i (dB), and the System Parameter ρ from Curve Fitting.

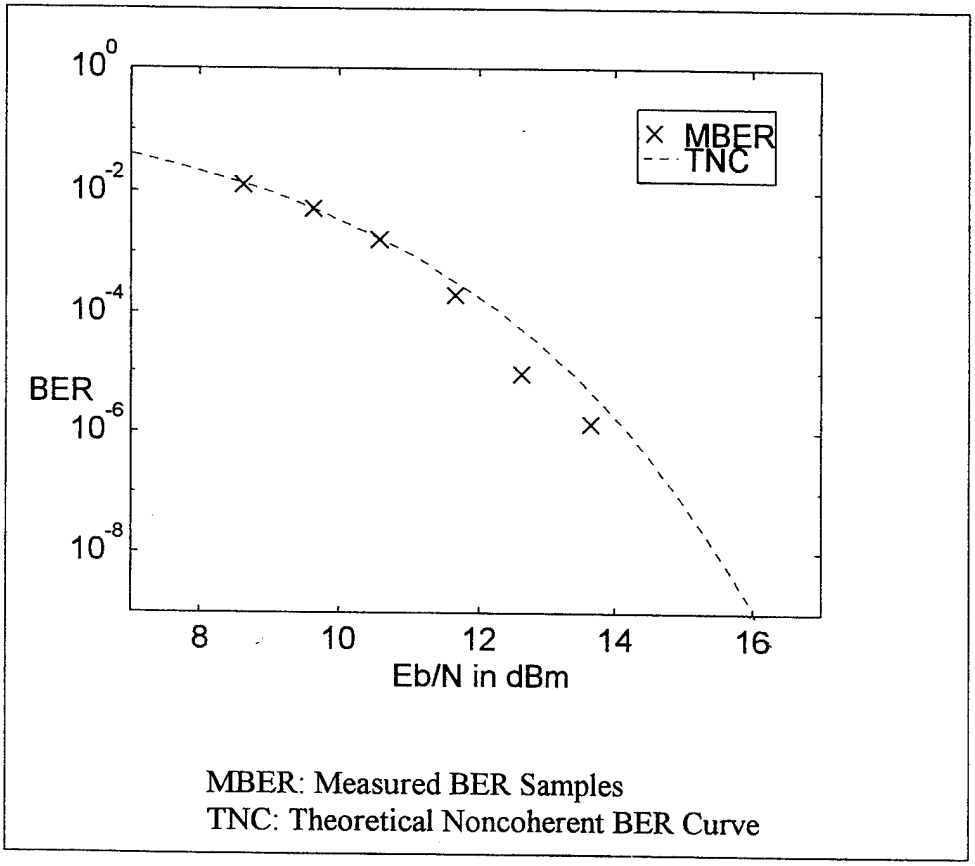

Figure 4.8. Measured BER Versus Variable Radiated Power with a Fixed Distance and a Fixed Jamming Power -17.0 dBm Compensated by System Parameter ρ.

In Table 4.6 with a -16.0 dBm jamming power, the parameter ρ is found to be 37.290 dBm, and the mean square error is 1.981×10^{-6}. The measured BER samples adjusted using the results of curve fitting procedure are shown in Figure 4.9.

jamming power	-16.0 dBm					
i	1	2	3	4	5	6
L_i (dB)	29.23	28.22	27.26	26.17	25.21	24.2
collection period (sec)	120	60	60	120	360	600
measured mean BER	2.10×10^{-2}	5.73×10^{-3}	2.08×10^{-4}	1.06×10^{-5}	1.02×10^{-6}	2.80×10^{-5}
ρ (dBm)	37.390					
MSE	1.891×10^{-6}					

Table 4.6. Mean BER Measurement at Different Attenuation L_i (dB), and the System Parameter ρ from Curve Fitting.

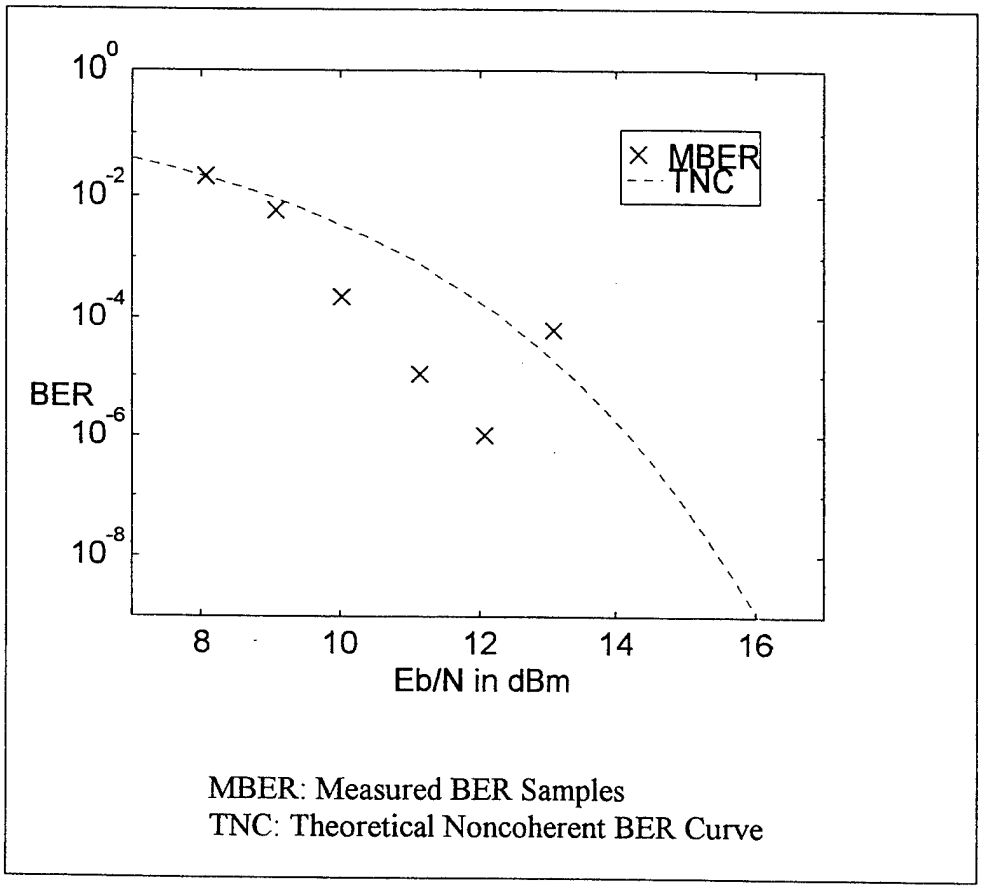

Figure 4.9. Measured BER Versus Variable Radiated Power with a Fixed Distance and a Fixed Jamming Power -16.0 dBm Compensated by System Parameter ρ.

From Table 4.4, 4.5, and 4.6 we obtain the different system parameters ρ as affected by various levels of jamming power. These values and the jamming powers are shown in Table 4.7.

parameter ρ	38.79	37.84	37.29
jamming power	-18.5 dBm	-17.0 dBm	-16.0 dBm

Table 4.7 Jamming Power and Parameter ρ.

Based on equation 3.18 and in the same communication environment, added jamming noise increases the noise figure *NF* of the system. The mean BERs increase with the jamming noise. After the curve fitting procedure, the parameter ρ is found to decrease with increasing jamming power. We would expect that the difference between different ρ's be equal to the difference between the different jamming powers, but the results do not show this. The higher the jamming power, the lower the value of ρ. Because the unknown interference may have changed the strength of the jamming noise, in our experiments the parameter ρ decreases with increasing jamming power.

E. FIXED STEP POWER CONTROL ALGORITHM

The measured BERs at the receiver were sent to the computer at the transmitter via the telephone line and modem where a fixed step power control algorithm written in LABVIEW was performed. Power control is performed in the experiments with and

without the presence of jamming noise. It is our objective to obtain the response of the algorithm on the transmitter side without jamming noise. It is also interesting to obtain the response of the fixed step power control algorithm in the presence of jamming noise. The results of the experiments and the features of the fixed step power control algorithm are now shown.

1. Fixed Step Power Control Algorithm

There is a required BER that is expected for in the link. This is referred to as BER_r. In the experiment, we can obtain the measured BER, BER_m, during a collection period. The algorithm of fixed step power control compares the relationship between BER_m and BER_r. Based on the result, the algorithm sends $L_i(n+1)$, the next attenuation, to the digital step attenuator. The algorithm of fixed step power control works in the following way:

- If BER_m is greater than BER_r, the transmitting power is too low. In this case, the algorithm sends $L_i(n+1) = L_i(n) - 1$ to the digital step attenuator to increase the radiated power .
- If BER_m is less than BER_r, the transmitting power is too high. In this case, the algorithm sends $L_i(n+1) = L_i(n) + 1$ to the digital step attenuator to decrease the radiated power.

2. Experiments of Fixed Step Power Control

Two experiments were performed: the fixed step power control without and with jamming noise. For the experiment without jamming noise, it is interesting to obtain the response of the control algorithm and the error status. For the experiment with jamming noise, we want to determine the sensitivity of the algorithm for fixed step power control. In these experiments the collection period was set to 20 seconds and BER_r was set to $1x10^{-3}$. This is equivalent to an error count of 384. The distance of the digital link was 59.5m. The initial attenuation on the digital step attenuator was set to zero.

3. Fixed Step Power Control Without Jamming Noise

For the experiment without jamming noise, we measure the response of the attenuator and the error count. This experiment was performed during 0000 to 0200 hours. We expect that the error count will increase to a level of 384 and then oscillate around this level. The attenuation will increase from zero to a stable value, decreasing the radiated power, until the error count is around 384. Figure 4.10 shows that the initial error is zero; and after thirty-four periods of collection time, the error oscillates around the level of error 384. The attenuation is increased in 0.5 dB increments. As can be seen in Figure 4.11, after thirty-four periods of collection time, the attenuation oscillates between 35 and 36. This is as expected.

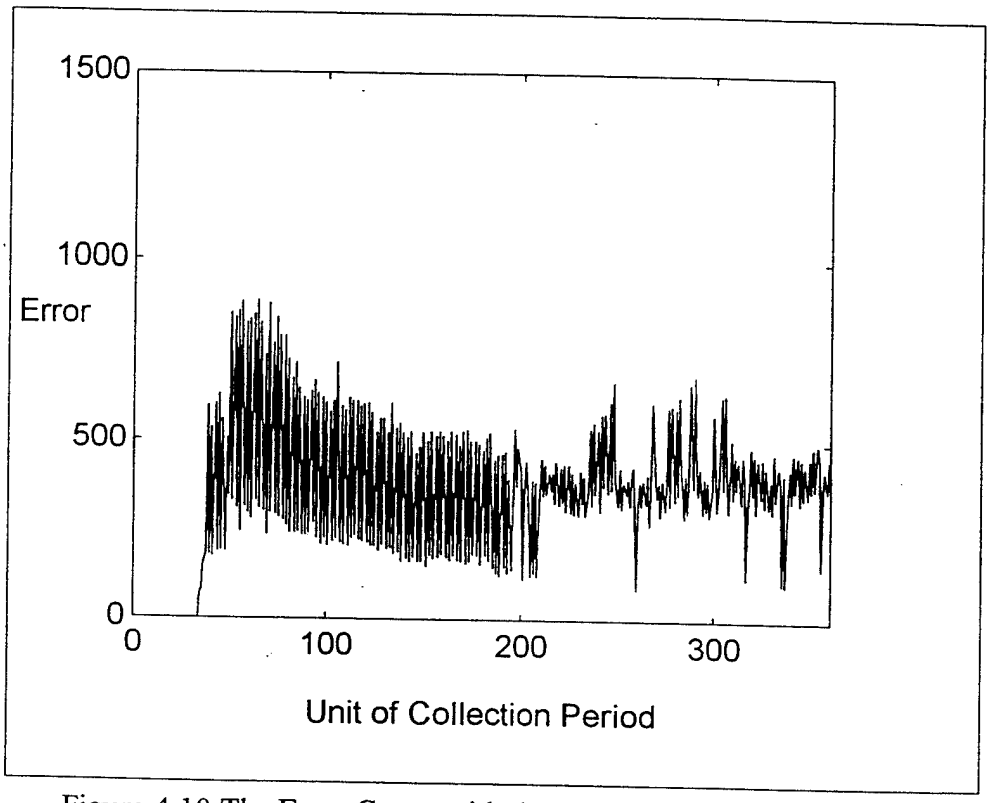

Figure 4.10 The Error Count with the Unit of Collection Time for a Fixed Step Control Algorithm.

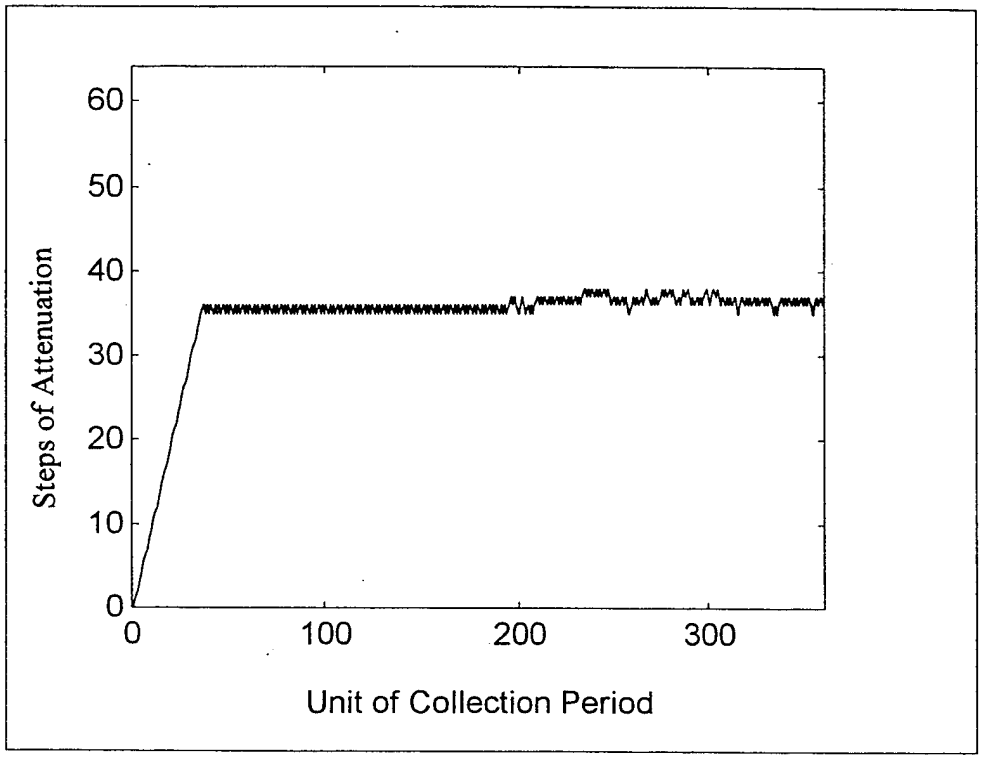

Figure 4.11 The Step of Attenuation with the Unit of Collection Period for a Fixed Step Control Algorithm.

4. Fixed Step Power Control With Jamming Noise

In the experiment with jamming noise, we expect to measure the attenuator response of the fixed step power control algorithm with different levels of jamming noise. We predict that the result of the error count before jamming will be the same as that in Figure 4.10. When the jamming noise is added, the error count should increase and the attenuation should decrease until the transmitting power is greater than the jamming noise power. At this point, we expect that the error count will oscillate around 384 as before. From equation 3.17, the difference of the two attenuations with two different jamming powers will be equal to the difference of the two jamming powers.

Figure 4.12 shows that the initial error is zero; and after 40 units of collection period, the error increases and shifts back to the level of error count 384. When a jamming power of -15 dBm is added, the error count increases to a peak of 3.2×10^4. When a jamming power of -21 dBm is added, the error increases to a peak of 1.1×10^4. When the jamming noise is turned off, the error count is low and the attenuation increases to the same value as that before the jamming noise was added. Figure 4.13 shows that, after 40 periods of collection time, the steps of attenuation shift between an attenuation of 40 and 41 without jamming noise. When a jamming power of -15 dBm is added, the attenuation decreases to 28 or 29. When a jamming power of -21 dBm is added, the attenuation decreases to 34 or 35. When the jamming noise is turned off, the attenuation increases to the same value as before. The error count is close to what is expected. Attenuation is incremented in 0.5 dB steps. The difference of the two

attenuations observed on the digital step attenuator with different jamming powers is not equal to the difference of the two jamming powers but is only half of the expected value. Presently, only a proportional change of the attenuation is verified in the experiment. Further study may be necessary in the future.

5. The Features for Fixed Step Power Control Algorithm

Based on the results shown in Figure 4.10, 4.11, 4.12, and 4.13, we obtain the features for the fixed step power control algorithm. Although the fixed step power control algorithm can perform the task of power control, it is not ideal. First, the fixed step power control algorithm attenuation is increased or decreased by one 0.5 dB step at a time. This takes too long to achieve the stable state required to overcome interference. Second, the reaction of the algorithm is slow. It cannot respond to interference periods that are shorter than the collection period. Finally, the difference of the two attenuations observed on the digital step attenuator with two different jamming powers is not equal to the difference of the two jamming powers. Further study of this is necessary.

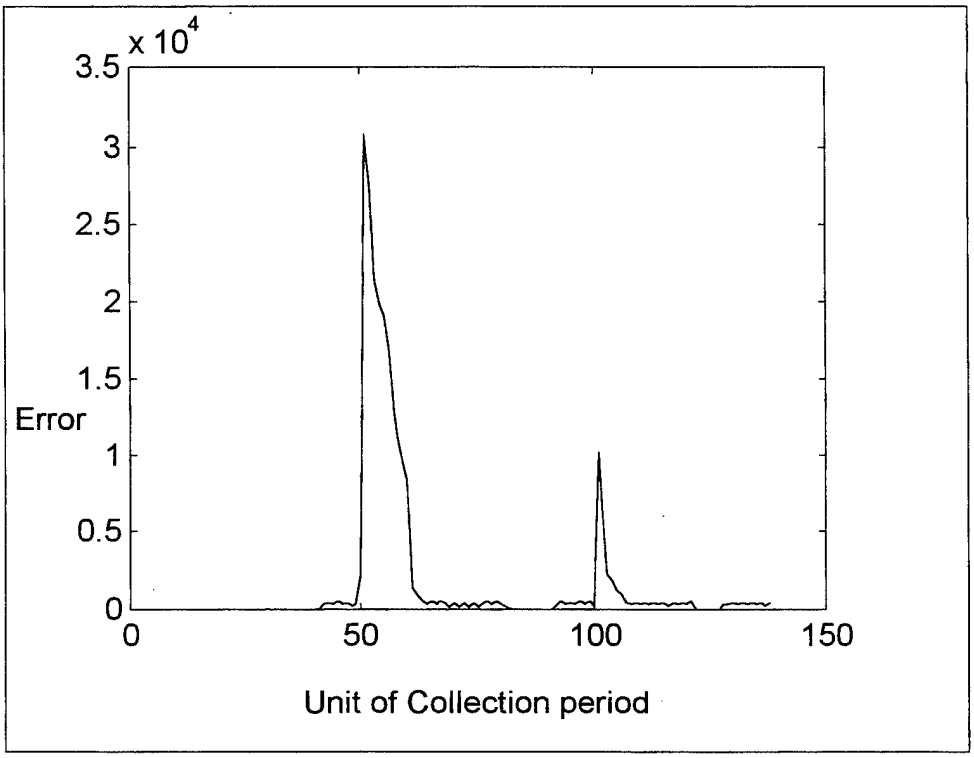

Figure 4.12. The Error with Jamming Noise Versus the Period of Collection Time.

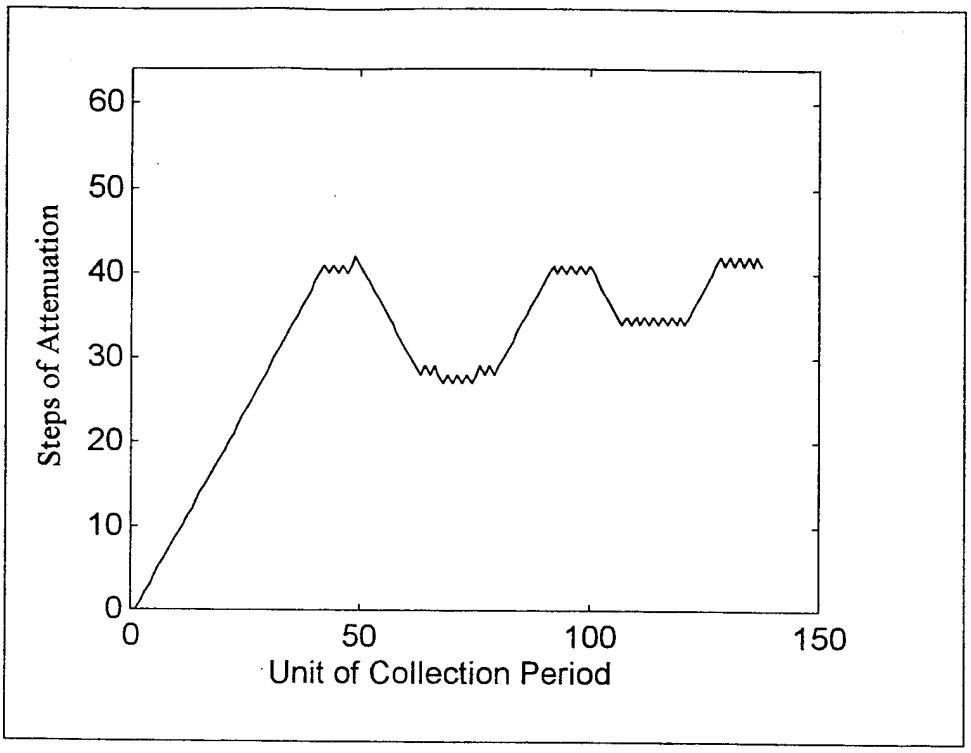

Figure 4.13 The Attenuation Value With the Unit of Collection Period For A Fixed Step Control Algorithm.

V. EXPERIENCE AND RECOMMENDATION

During the various experiments, much time was spent solving practical problems. Here we describe some problems and recommendations for improvement. This may be helpful to future experimenters in this subject area. One problem we encountered relates to the coaxial cable. Another relates to the problems due to interference and multipath.

To perform these experiments, we put all system components inside except the antenna, which was on the roof. This offers three advantages: convenience when collecting data for a long time, reduction in equipment damage, and reduction in the error resulting from movement. One disadvantage is the increased attenuation resulting from a long co-axial cable. We encountered two problems concerning the co-axial cable connection to the antenna.

A. STANDING WAVE RATIO (SWR) MEASUREMENT

Before connecting the co-axial cable to the antenn, the SWR of the co-axial cable must be measured. The power supply of the transmitter/receiver should be connected to a stable 12V dc power supply. In earlier experiments, we used a portable 12V dc battery. In this instance, the SWR measurements were different every time because the voltage of the battery was insufficiently stable. In later experiments, when a stable voltage source was used, the SWR measurement was stable and reliable.

B. CABLE MATCHING

Before connecting the co-axial cable from the transmitter to the antenna, the co-axial cable must be matched with the antenna impedance. Ideally, the value of the SWR should be unity. Trial and error methods were used for lengths of $\lambda/4$, $\lambda/2$, $3\lambda/4$, as well as integer multiples wavelength (λ) of the co-axial cable. The value of SWR is the least and approaches unity when the length of the co-axial cable is equal to an integer multiple of λ.

C. EXPERIMENTAL ENVIRONMENT RECOMMENDATIONS

The experiments were critically affected by unknown interference. To avoid unknown interference, it is best to perform the experiments in an anechoic chamber. In this ideal environment, the results should match what we expect from theory. At this time, no anechoic chamber in UHF range is available.

VI. CONCLUSIONS

In an ideal thermal noise limited receiver, E_b/N_0 measured at the detector input determines the detection quality. In a nonideal noisy receiver, E_b/N determines the detection quality. Both the dependency of the logarithm of BER versus the logarithm of E_b/N_0 and the dependency of the logarithm of BER versus the logarithm of E_b/N were shown. We know that the BER of a noisy receiver is actually a shifted function of the BER of an ideal thermal noise limited receiver along the logarithm of E_b/N_0 axis.

The measurement of BER with a fixed power at a fixed location was performed. The results showed the effect of propagation and interference. Based on the results, a decision was made that the experiments should be performed during the period with the least interference (0000 hours to 0800 hours) to get more stable results.

We tried to obtain the relationship between BER and communication distance with fixed radiated power, but the signal strength between two locations is in practice very complicated because of unknown interference and multipath effects. This result suggested that varying distance in our experiments for measurement was not a viable approach.

In order to implement the power control algorithm, it is necessary to characterize the radio link by the system parameter ρ. Due to the many interferences possible, it is very difficult to obtain the system parameter ρ directly. Therefore, we introduced a curve fitting search procedure. Three sets of data were collected in the experiments

without a jammer. The measured mean BERs were then used in the curve fitting procedure to find the system parameter ρ. These experimental results showed that the curve fitting procedure is a very stable process by which find the parameter ρ even in a noisy environment. We repeated the experiment with different amounts of jamming noise injected into the system as well. The difference between ρ obtained with and without the jammer should be equal to the difference between jamming power. The difference of the two attenuations observed on the digital step attenuator with different jamming powers is not equal to the difference of the two jamming powers but is only half of the expected value. The parameter ρ did change in proportion to the power of jamming noise. The higher the jamming power, the lower the value of the parameter ρ. In these experiments, the unknown interference is one of the critical factors that affect the experimental results. If these experiments can be performed in an anechoic chamber, the interference and multipath problems can be avoided.

The fixed step power control algorithm was implemented. Its reaction response time to a jammer is too slow. When interference is present, it takes too long to react to the interference. The power always increases or decreases one step in the algorithm. The results showed the BER quality shifting up and down relative to the desired level. These problems can be solved by an adaptive power control algorithm. Measuring the system parameter ρ is an important step in the design of a power control algorithm.

APPENDIX

This is the cable program used in the error counter.

```
MODULE  count_up
TITLE               '22V10 PROGRAM that counts'
U3                  DEVICE  'P18CV8'

" input pins of P22V10
   CLK              PIN    1;
   en               PIN    2;
   CLR              PIN    3;

"output pins of P22V10
Q3,Q2,Q1,Q0,Q7,Q6,Q5,Q4              PIN      19,18,17,16,15,14,13,12;

Q3,Q2,Q1,Q0,Q7,Q6,Q5,Q4              IsType   'feed_reg,reg_D,pos';

EQUATIONS

Q0 := (en & Q0) # (!en & (!Q0));
Q1 := (en & Q1) # (!en & ((Q1$Q0) & !Q3 # (Q2&Q3) # (Q3&Q1)));
Q2 := (en & Q2) # (!en & ((!Q3&!Q2&Q1&Q0) # (Q2&!Q1) # (Q2&!Q0)));
Q3 := (en & Q3) # (!en & (Q2&Q1&Q0) # (Q3&!Q1&!Q0);

Q4 := (en # !(Q0&Q3))&Q4) # (!en & (Q0&Q3)&(!Q4));
Q5 := (en&Q5) # (!en & ((Q0$Q3) & (!Q7&!Q5&Q4)) # (!Q4&Q5) #
      (!(Q3&Q0)&Q5);
Q6 := ( Q6& ( en # !(Q0&Q3) # (!Q5) # (Q5 & !Q4) ) # (!Q4&Q5) #
      (!(Q0&Q3)  & Q5);
Q7 := (!en&(Q0&Q3)&!Q7&Q6&Q5&Q4)#(Q7&(en#!(Q3&Q0))) #
      (Q7&!Q6&!Q5&!Q4);

"RESET
        [Q0.RE,Q1.RE,Q2.RE,Q3.RE,Q4.RE,Q5.RE,Q6.RE,Q7.RE]=CLR;

TEST_VECTORS ( [CLK,en,CLR] -> [Q7,Q6,Q5,Q4,Q3,Q2,Q1,Q0] )
                    [  0,   0,   0 ] -> [  0,  0,   0,  0,  0,  0,  0,  0 ];
                    [  .c.  0,   0 ] -> [  0,  0,   0,  0,  0,  0,  0,  1 ];
                    [  .c.  0,   0 ] -> [  0,  0,   0,  0,  0,  0,  1,  0 ];
```

```
[ .c.   0,   0 ] -> [ 0,  0,   0,  0,  0,  0,  1,  1 ];
[ .c.   0,   0 ] -> [ 0,  0,   0,  0,  0,  1,  0,  0 ];

[ .c.   0,   0 ] -> [ 0,  0,   0,  0,  0,  1,  0,  1 ];
[ .c.   0,   0 ] -> [ 0,  0,   0,  0,  0,  1,  1,  0 ];
[ .c.   0,   0 ] -> [ 0,  0,   0,  0,  0,  1,  1,  1 ];
[ .c.   0,   0 ] -> [ 0,  0,   0,  0,  1,  0,  0,  0 ];

[ .c.   0,   0 ] -> [ 0,  0,   0,  0,  1,  0,  0,  1 ];
[ .c.   0,   0 ] -> [ 0,  0,   0,  1,  0,  0,  0,  0 ];
[ .c.   0,   0 ] -> [ 0,  0,   0,  1,  0,  0,  0,  1 ];
[ .c.   1,   0 ] -> [ 0,  0,   0,  1,  0,  0,  0,  1 ];
[ .c.   0,   1 ] -> [ 0,  0,   0,  0,  0,  0,  0,  0 ];
END count_up
```

LIST OF REFERENCES

1. Kumar, P. Sarath, Yates, Roy D., and Holtzman, Jack, "Power control based on Bit Error Rate (BER) measurements," Proc. of MILCOM95, vol. 2, pp. 617- 620, 1995.

2. Kumar, P. Sarath and Holtzman, Jack, "Analysis of Handoff Algorithms Using both Bit Error Bate (BER) and Relative Signal Strength," Proc. Int. Conf. Universal Personal Communications, pp. 1-5, Oct. 27-Nov. 1, 1994.

3. Chockalingam, A. and Milstein, Laurence B., "Closed-Loop power control performance in a cellular CDMA system," Proc. of MILCOM95, vol. 3, pp. 937- 941, 1995.

4. *Kantronics Data Engine Operator's Manual*, Kantronics Co., Inc., Lawrence, KA, 1990.

5. *DE19K2/9K6 Modem Owner's Manual*, Kantronics Co., Inc., Lawrence, KA, 1991.

6. *D4-10 UHF Wide-Band Transceiver Operator's Manual*, Kantronics Co., Inc., Lawrence, KA, 1991.

7. Brooke, A., Kendrick, D., and Meeraus, A., *GAMS: A User's Guide, Release 2.25*, Boyd & Fraser Publishing Co., Danvers, MA, 1992.

8. Freeman, Roger L., *Telecommunication transmission handbook third edition*, John Wiley & Sons, Inc., New York, 1991.

INITIAL DISTRIBUTION LIST

		No. Copies
1.	Defense Technical Information Center 8725 John J. Kingman Road, Ste 0944 Alexandria, VA 22060-6218	2
2.	Dudley Knox Library Naval Postgraduate School 411 Dyer Road Monterey, CA 93943-5101	2
3.	Prof. Herschel H. Loomis,Jr., Code EC/Lm Department of Electrical and Computer Engineering Naval Postgraduate School Monterey, CA 93943-5121	1
4.	Prof. Chin-Hwa Lee, Code EC/Le Department of Electrical and Computer Engineering Naval Postgraduate School Monterey, CA 93943-5121	3
5.	Prof. R. Clark Robertson, Code EC/Rc Department of Electrical and Computer Engineering Naval Postgraduate School Monterey, CA 93943-5121	1
6.	Prof. Ramakrishna Janaswamy, Code EC/Js Department of Electrical and Computer Engineering Naval Postgraduate School Monterey, CA 93943-5121	1
7.	LCDR Hsu, Hsien-Ming No. 14-1 Lane 139 Tsoying Big Road Kaohsiung, Taiwan Republic of China	2